Expression Microdissection

Operator-Independent Retrieval of Cells for Molecular Profiling

Michael A. Tangrea, PhD, Rodrigo F. Chuaqui, MD,* John W. Gillespie, MD,*† Mamoun Ahram, PhD,* Gallya Gannot, DMD, PhD,* Benjamin S. Wallis, BA,* Carolyn J. M. Best, PhD,* W. Marston Linehan, MD,‡ Lance A. Liotta, MD, PhD,§ Thomas J. Pohida, PhD,‖ Robert F. Bonner, PhD,¶ and Michael R. Emmert-Buck, MD, PhD**

Abstract: Tissue microdissection is an important method for the study of disease states. However, it is difficult to perform high-throughput molecular analysis with current techniques. We describe here a prototype version of a novel technique (expression microdissection) that allows for the procurement of desired cells via molecular targeting. Expression microdissection (xMD) offers significant advantages over available methods, including an increase in dissection speed of several orders of magnitude. xMD may become a valuable tool for investigators studying cancer or other disease states in patient specimens and animal models.

Key Words: expression microdissection, immunohistochemistry, genomics, proteomics

(*Diagn Mol Pathol* 2004;13:207–212)

Tissue microdissection has advanced significantly over the past decade, from crude slide-scraping tools to sophisticated laser-based instruments.[1–13] In combination with high-throughput molecular analysis methods, it is now theoretically possible to generate whole genome/proteome profiling data from specific cell populations procured from human or animal tissues.[14] However, it is clear that current microdissection techniques are not sufficient to fully support the study of genomics and proteomics. In particular, there is a frequent mismatch between the number of cells of interest that can be realistically procured versus the number required for many downstream analyses. In order for tissue microdissection to keep pace with the needs of investigators, it is important that simpler and faster approaches are contemplated and developed.

Here we present a novel technique, expression microdissection (xMD), which removes the "human element" from the process by employing a targeting probe as the workhorse of the system. In other words, the method converts microdissection from an operator-dependent to an operator-independent mode, thus eliminating the need to laboriously procure cells. xMD recovers target cells using standard immunohistochemical (IHC) staining procedures, thermoplastic film, and a light source as diagrammed in Figure 1. An ethylene vinyl acetate (EVA) polymer film coating is placed on top of a conventional, non–cover-slipped immunostained tissue section. Unlike laser capture microdissection (LCM), the film does not contain a light absorbing dye, rather the light energy passes unattenuated through the EVA film and is absorbed only where there is a strong deposition of highly absorbing immunostain. The stain then heats the overlying clear polymer, causing it to focally melt. Below this staining threshold (which is dependent on the absorbed light energy density or fluence), the overlying film is not affected. The thermoplastic bond is formed only with cells (or organelles) exceeding the stain threshold concentration, thus the selection of captured cells is determined wholly by immunobased targeting. No visualization of cells or use of microscopes is required.

Potentially, xMD offers several advantages over current methods, including (1) increased dissection rate (several orders of magnitude), (2) increased dissection precision (subcellular), (3) removal of variance among individual operators, permitting standardization of the dissection process, and (4) elimination of targeting difficulties due to poor image quality of non–cover-slipped (non–index-matched) histology sections used in current dissection systems. In the present report, we describe reduction-to-practice of xMD and demonstrate the utility of a prototype version of the method for a variety of biologic applications.

From the *Pathogenetics Unit, Laboratory of Pathology and Urologic Oncology Branch, Center for Cancer Research, National Cancer Institute, Bethesda, Maryland; †Science Applications International Corporation, Frederick, Maryland; ‡Urologic Oncology Branch, Center for Cancer Research; §Laboratory of Pathology, Center for Cancer Research, ‖Signal Processing and Instrumentation Section, Computational Bioscience and Engineering Laboratory, National Cancer Institute, Bethesda, Maryland; and ¶Laboratory of Integrative and Medical Biophysics, National Institute for Child Health and Human Development, Bethesda, Maryland.

Reprints: Michael R. Emmert-Buck, MD, PhD, National Cancer Institute, Advanced Technology Center 8717 Grovemont Circle, Gaithersburg, MD 20878 (e-mail: buckm@mail.nih.gov).

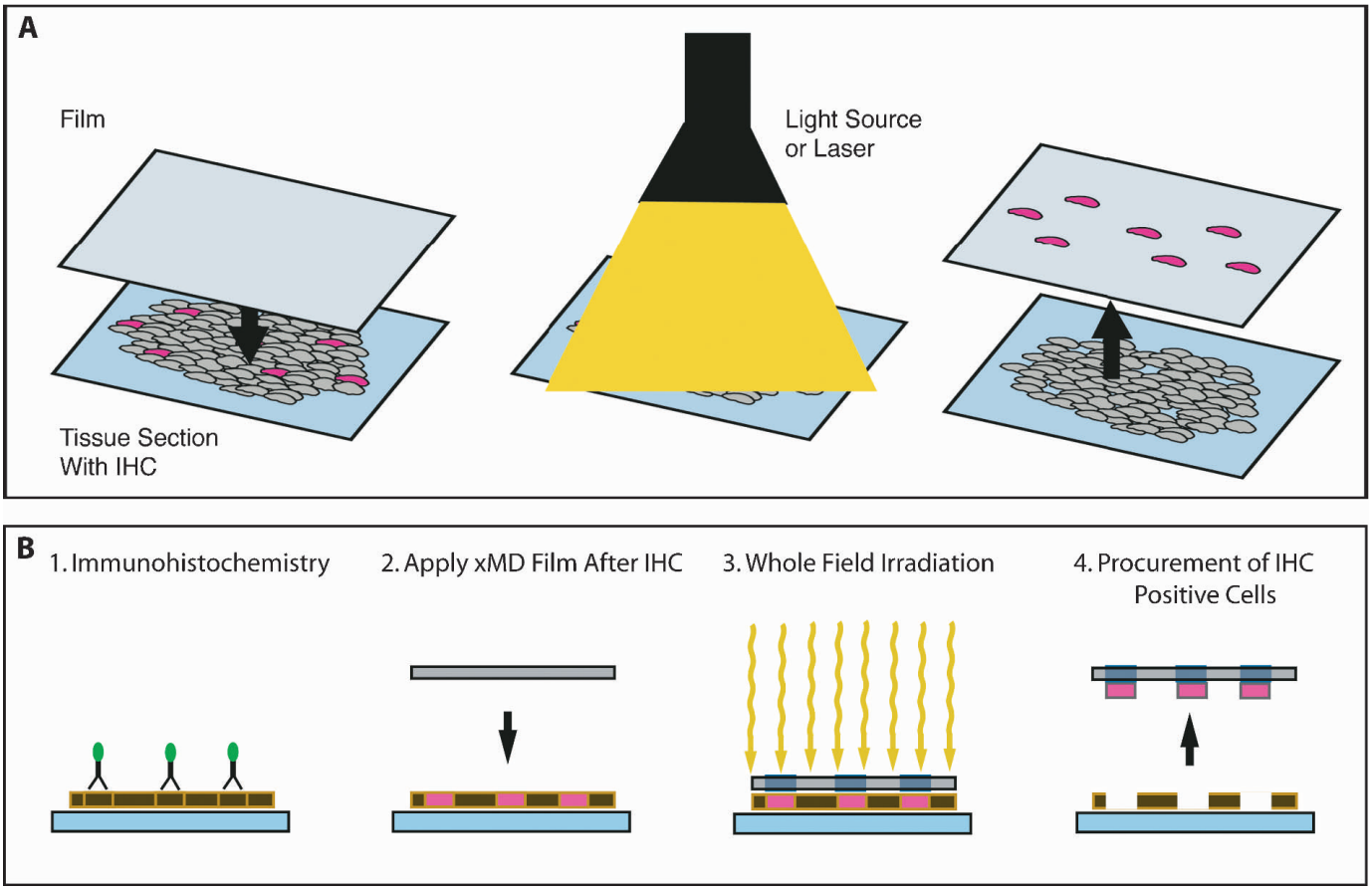

FIGURE 1. Schematic illustrations of expression microdissection (xMD). A, Overview of the xMD method using a flashlamp light source. Cells highlighted in magenta represent those targeted by immunohistochemistry (IHC). B, Detailed stepwise schematic of xMD. IHC targeting molecules (inverted "Y") are attached to the labeling enzyme (green sphere).

MATERIALS AND METHODS

Tissue Specimens

Patient tissue samples were obtained from Institutional Review Board (IRB)–approved clinical protocols and subsequently anonymized. Formalin-fixed, paraffin-embedded, ethanol-fixed paraffin-embedded, as well as frozen tissues, were dissected and subsequently analyzed.

1. Formalin-fixed, paraffin-embedded tissue: proliferating cell nuclear antigen (PCNA) (Zymed Laboratories, South San Francisco, CA, prediluted) positive nuclei from mouse colon tissue and cytomegalovirus (CMV) (DAKO/Cytomation, Carpinteria, CA, 1:10 dilution with antigen retrieval) positive cells from human lung tissue were dissected. The DNA from PCNA procured nuclei was amplified using the glyceraldehyde 3-phosphate dehydrogenase (GAPDH) primer set.
2. Ethanol-fixed, paraffin-embedded tissue: human prostate tissue was used for dissection studies using the following antibodies: cytokeratin AE1/AE3 (DAKO/Cytomation, Carpinteria, CA, 1:50 dilution), CD3 (Zymed Laboratories, South San Francisco, CA, prediluted), prostate-specific antigen (PSA)(Zymed Laboratories, South San Francisco, CA, prediluted), desmin (Zymed Laboratories, South San Francisco, CA, prediluted), S-100 (Zymed Laboratories, South San Francisco, CA, prediluted), glyceraldehyde 3-phosphate dehydrogenase (GAPDH) (Biogenesis, Kingston, NH, 1:10 dilution), e-cadherin (Transduction Laboratories, Lexington, KY, 1:500 dilution), smooth muscle actin (SMA) (Zymed Laboratories, pre-diluted), vimentin (DAKO/Cytomation, Carpinteria, CA, 1:40 dilution), histone (NeoMarkers, Fremont, CA, 1:20 dilution). In addition, DNA from xMD procured cytokeratin positive cells was also analyzed by the amplification of three sequence tagged site markers, and via allelotyping at microsatellite marker D8S1786.
3. Frozen tissue: smooth muscle actin (SMA) (Zymed Laboratories, prediluted) positive cells and cytokeratin AE1/AE3 (DAKO/Cytomation, Carpinteria, CA, 1:50 dilution) positive cells were dissected from human prostate tissue. Both protein and RNA analysis were performed with these dissections. RT-PCR and protein analysis was com-

pleted with SMA positive and cytokeratin AE1/AE3 positive cells from human prostate.

Immunhistochemistry

Five-micron thick histologic sections were mounted on uncharged slides. Prior to immunohistochemistry, the tissue was de-waxed and rehydrated following standard techniques. The DAKO Envision$^+$ System with diaminobenzidine (DAB) (DAKO/Cytomation, Carpinteria, CA) was used as the method for immunohistochemistry following the manufacturer's instructions, except the DAB stain was 3X concentrated and the incubation time was extended from 10 to 20 minutes. The slides were not counterstained to enhance the contrast between stained areas and unstained areas. The non–cover-slipped sections were dehydrated through graded alcohols and xylenes and then allowed to air dry. A previously described abbreviated immunohistochemistry protocol was used for frozen tissue sections to optimize the preservation of the RNA and protein quality.[15]

Expression Microdissection (xMD)

xMD was performed with two separate laser systems. In all experiments, the entire histologic field was irradiated, except in the case of the proliferating nuclear cell antigen (PCNA) stained sections, where the laser was specifically directed to the highlighted area represented by the red rectangle (Fig. 2H). Laser system #1 was an Arcturus PixCell II with the following parameters: power = 100 mW, duration = 30-40 milliseconds, repeat t = 1.2 seconds, target = 0.300 V, current = 25.0 mA, spot size = 30 μm, and temperature = 24°C. Laser system #2 was a 400 mW fiber optic LD diode source with a 200 μm spot size, scanned in the continuous mode at ~3 cm/s, using a motorized slide stage.

Analysis of DNA

After dissection, DNA was extracted as previously described.[5] Primer sets were used for three STS markers, *WI-3279, WI-16152,* and *WI-17142* (Research Genetics, Inc, Carlsbad, CA); four polymorphic DNA markers for allelotyping at chromosome 8p21 (*D8S136, D8S1836, D8S137,* and *D8S1733*) (Research Genetics, Inc, Carlsbad, CA); and murine GAPDH. For the 8p microsatellite markers, [^{33}P]-labeled DNA was denatured and electrophoresed on acrylamide gels at 1,800 volts for 1.5 hours. For the STS markers and GAPDH primers, products were electrophoresed in 1.5% agarose gels and visualized with ethidium bromide staining.

Analysis of RNA

After dissection, total RNA was isolated using the PicoPure RNA Isolation Kit (Arcturus, Mountain View, CA), following manufacturer's instructions. The final volume of RNA was 15 μL per sample. For each sample, 2 μL of RNA were used to perform a positive RT and 2 μL for a negative RT (no reverse transcriptase) as previously described.[16] RT-PCR products were electrophoresed in 1.5% agarose gels and visualized with ethidium bromide staining.

Analysis of Proteins

Proteins were eluted from the xMD film in 50 μL of RIPA lysis buffer (Upstate, Charlottesville, VA) containing Complete Protease Inhibitor (Roche, Basel Switzerland). The protein extraction samples were electrophoresed in a 4% to 20% Tris-Glycine gel (Invitrogen, Carlsbad, CA) at a constant voltage of 125 V for 1.5 hours and visualized with SilverQuest Silver Stain (Invitrogen, Carlsbad, CA) according to manufacturer's instructions. Immunoblot analysis for mouse anti–α-tubulin (Sigma, St. Louis, MO) was completed using previously described methodology.[17] Proteins were visualized with ECL Immunoblotting Kit (Amersham, Piscataway, NJ) according to manufacturer's instructions.

RESULTS AND DISCUSSION

The first experiments were performed to assess the physical principles underlying xMD, including laser dosimetry (wavelength, power, and pulse time and number), transfer film characteristics, cellular stains, and heat sink effects of tissue section support surfaces. An optimized protocol was developed to maximize film activation and adherence to the underlying substrate. The method was then applied to histologic sections to evaluate the process. Twelve antibodies were tested. In each case where cellular staining was observed, the labeled cells were successfully retrieved. Importantly, no film activation occurred in nontargeted regions of the tissue, and the technique worked effectively on histology slides prepared from snap-frozen tissue, formalin-fixed, paraffin-embedded specimens and ethanol-fixed paraffin-embedded samples. The transfer film used for LCM and xMD undergoes a distinct change in appearance during the dissection process as the EVA expands due to thermal activation. Once the intervening air space is removed and EVA bonds the underlying tissue, the microscopic image becomes index matched and the dissection region is clearly identifiable. Thus, during development of xMD, we were able to visually monitor the dissection process and establish laser parameters that resulted in precise procurement of targeted cells. Inadvertent recovery of nontarget cells did not occur; we examined this phenomenon in detail and observed that activation of transfer film does not take place in the presence of immunohistochemical background staining.

Figure 2A demonstrates recovery of prostate glands from a human tissue section onto transfer film using cytokeratin as a targeting antibody. The epithelium from a 10 mm^2 area (approximately 100,000 cells) was precisely microdissected using a prototype scanning laser xMD system that operates at a dissection rate of approximately 4,000 cells per second. Panels B and C show a section of prostate epithelium

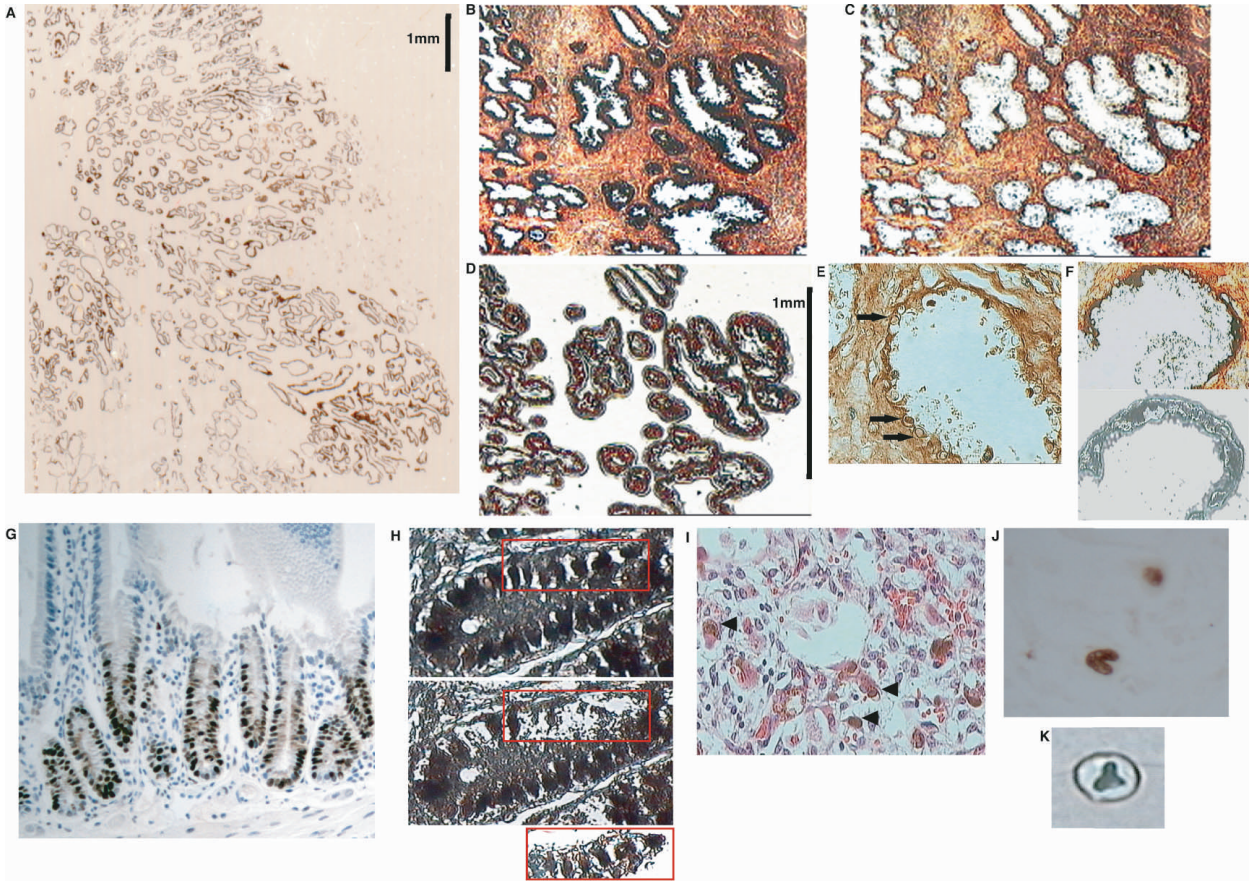

FIGURE 2. Procurement of specific cell types using xMD. A, xMD transfer film of an entire field of ethanol-fixed paraffin-embedded human prostate epithelium dissected using anti-cytokeratin as a targeting antibody, 10× magnification. B-D, Dissection of ethanol-fixed, paraffin-embedded human prostate epithelium stained for prostate-specific antigen (PSA), before (B) and after xMD (C). Both (B) and (C) are non–cover-slipped tissue images. Cells recovered onto transfer film (D). All 3 images are 20× magnification. (E) Basal epithelial cells (highlighted by arrows) from ethanol-fixed, paraffin-embedded human prostate tissue after procurement of PSA positive secretory cells with xMD, 400× magnification, cover-slipped image. F, Isolation of basal epithelial cells from ethanol-fixed, paraffin-embedded human prostate tissue after procurement of PSA positive secretory cells with xMD, 400× magnification. Upper panel, non–cover-slipped basal epithelial cell image. Lower panel, isolated basal epithelium cells on transfer film. G, Representative formalin-fixed paraffin-embedded mouse colon section showing proliferating nuclear cell antigen (PCNA) positive nuclei of cells in lower segment of crypts, 200× magnification, cover-slipped image. H, xMD procurement of PCNA-positive nuclei from formalin-fixed, paraffin-embedded mouse colon tissue, 400× magnification. Two upper panels display non–cover-slipped images of mouse colon tissue, before and after dissection. Area of dissection indicated by red rectangle. Lower panel, PCNA-positive nuclei on xMD transfer film. I, A standard hematoxylin and eosin–stained cytomegalovirus (CMV) infected formalin-fixed, paraffin-embedded human lung section with characteristic nuclear viral inclusions highlighted by arrowheads, 400× magnification, cover-slipped image. J, Representative CMV-positive nuclei immunostained with diaminobenzidine (DAB), shown without counterstain, 400× magnification, coverslipped image. K, xMD transfer film of a CMV infected nuclei from formalin-fixed, paraffin-embedded human lung tissue, 400× magnification.

stained with an antibody against prostate-specific antigen (PSA), before (Fig. 2B) and after (Fig. 2C) xMD. The procured cells are displayed on the transfer film in Figure 2D.

Since activation of the film is specifically localized to the region of dye deposition, xMD appears to be very precise. Close inspection of the dissected glands in Figure 2 indicates that only the inner PSA positive secretory cells were removed. The surrounding, PSA negative basal stem-cell layer (counterstained with hematoxylin and eosin) was not procured (Fig. 2E). The stem cells can be subsequently dissected using either standard LCM or potentially more rapidly (and accurately) with a second round of xMD using an antibody specific for basal cells, such as high–molecular-weight cytokeratin (Fig. 2F).[18] Determining the role(s) that secretory and basal stem cells play in normal prostate physiology and disease is of great interest; however, at present, it is extremely difficult to directly recover these cells from tissue sections. The wide range of antibodies available for immunohistochemical staining offers

many possibilities for xMD. For example, studies of normal prostate and prostate cancer could be extended by using commercially available antibodies that specifically target tumor cells, normal epithelial cells, neovessels, proliferating cells, apoptotic cells, infected cells, inflammatory cells, stromal cells, specific pathway-activated cells, p53 mutation-positive cells, or cells in a specific phase of the cell cycle. A useful feature regarding IHC absorptive stains is the intrinsically poor contrast that comes from attenuation of transmitted light. Only when the absorption is >50% is the contrast sufficient to visualize target cells through the microscope, the same amount of incident light required to activate the thermoplastic polymer. Thus, minimal set-up time is required to add a new antibody to a study since target cells will be efficiently procured if they are considered to be positively stained using standard IHC criterion.

Our experience to date indicates that xMD is capable of dissecting target structures smaller than a single cell, although we have not yet fully optimized this application in the laboratory. A histologic section of normal mouse colon stained for proliferating nuclear cell antigen (PCNA) shows positively stained nuclei in the lower segment of colonic crypts in Figure 2G. Superficial epithelium and upper segments of the glands are PCNA negative. Successful procurement of PCNA immunostained nuclei is demonstrated in Figure 2H. Similarly, dissection of cytomegalovirus (CMV) positive nuclei from infected human lung is possible using xMD. A standard hematoxylin and eosin–stained section is shown in Figure 2I with characteristic nuclear viral inclusions highlighted by arrowheads. CMV immunopositive nuclei are evident (Fig. 2J), and the recovered nuclei after xMD are shown on the transfer film in Figure 2K. Although dissection of subcellular structures is theoretically possible using currently available laser systems, targeting of these small structures is technically challenging and recovery of sufficient material (for example, hundreds of thousands of individually procured nuclei) for molecular analysis is problematic. In both the PCNA and CMV targeting experiments, three advantages of xMD are demonstrated: (1) precise subcellular dissection of nuclei, (2) expression-targeted dissection of a specific subset of nuclei, and (3) operator-independent dissection.

We performed several common laboratory methods on the recovered cells. DNA, mRNA, and proteins were individually analyzed. Similar to LCM, the cells are exposed to a brief thermal transient (5–10 milliseconds) during film activation; thus, it was important to determine if they are damaged during the process. This was an issue to which we paid particular attention and carefully evaluated during the initial development of LCM. Figure 3A demonstrates polymerase chain amplification (PCR) of DNA at three sequence-tagged sites (STS). In this example, xMD used cytokeratin-based targeting of ethanol-fixed, paraffin-embedded human prostate epithelium. Allelotyping of two patient samples using microsatellite marker

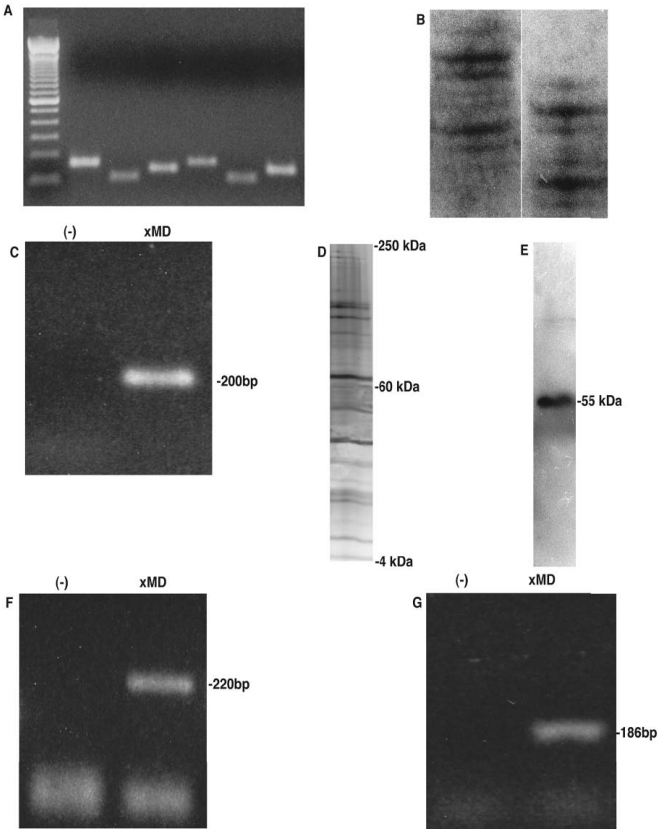

FIGURE 3. DNA, protein, and mRNA analysis after xMD. A, Amplification (in duplicate) of 3 sequence-tagged site markers using DNA derived from ethanol-fixed, paraffin-embedded human prostate epithelium. B, Allelotyping of ethanol-fixed, paraffin-embedded human prostate epithelial-derived DNA after xMD at microsatellite marker *D8S1786*. Two separate patients were analyzed both of whom were heterozygous at this locus. C, Amplification of DNA from formalin-fixed, paraffin-embedded mouse PCNA positive nuclei using a primer set for glyceraldehyde 3-phosphate dehydrogenase (GAPDH), (-) denotes the negative control. D, Analysis of total protein from smooth muscle actin (SMA) targeted cells from frozen human prostate by 1-dimensional polyacryalmide gel electrophoresis, followed by silver staining. E, Immunoblot for α-tubulin protein from cytokeratin-targeted frozen human prostate epithelium. F, RT-PCR of beta-actin mRNA from cytokeratin-targeted frozen human prostate epithelium, (-) denotes the negative control. G, RT-PCR of hypoxanthine guanine phosphoribosyl transferase (HPRT) from smooth muscle actin positive frozen human prostate stromal cells, (-) denotes the negative control.

D8S1786 was also performed on cytokeratin-targeted, ethanol-fixed, paraffin-embedded prostate epithelium (Fig. 3B). Amplification of the glyceraldehyde 3-phosphate dehydrogenase (GAPDH) gene was successful with DNA recovered from formalin-fixed, paraffin-embedded mouse colon PCNA positive nuclei (Fig. 3C). After xMD, protein lysates from frozen human prostate tissue were evaluated by 1D-PAGE (Fig. 3D,

smooth muscle actin-targeted cells) and by immunoblot for α-tubulin (Fig. 3E, cytokeratin-targeted cells). Neither protein quantity nor quality was adversely affected by xMD. Gene specific RT-PCR of mRNA was performed for β-actin from mRNA recovered from frozen human prostate epithelium using cytokeratin-targeted as shown in Figure 3F, and for hypoxanthine guanine phosphoribosyl transferase (HPRT) from smooth muscle stromal cell mRNA using actin as a targeting tool shown in Figure 3G.

In studies of tissue specimens, front-end processing steps (time interval to fixation or freezing, type of fixative, temperature levels during embedding) have a significant effect on downstream molecular analyses, especially for mRNA and protein applications. In addition to biomolecule degradation typically found with fixation, total protein yields from archived material is lower than that observed from frozen tissue samples.[19,20] For example, we have shown previously that significantly larger dissections from ethanol-fixed, paraffin-embedded tissue are necessary to obtain similar immunoblot data compared with frozen tissues.[19] To date, we have not observed any specific biomolecule degradation due to the xMD procurement process for either proteins or nucleic acids. The major limitation is the quality of the molecules in the starting material. Further automation of xMD may improve the quality of recovered biomolecules over alternative methods due to decreased dissection times.

One can envision multiple embodiments of xMD. The simplest approach is to immunostain a tissue section(s), cover the slide with transfer film, and irradiate the entire field with a flashlamp or with a scanning laser beam as described above. Employed in conjunction with an automated immunostainer, this allows rapid recovery of a large number of target cells. For example, a histologic section of a cancer sample typically contains several hundred thousand tumor cells (or more). Recovery of the entire cancer cell population from as many as 40 sequential tissue section recuts (>10^7 total cells) is possible in less than a day. Thus, investigators can study a dissected tumor cell population using analytic methods that have previously been impractical, such as those applied to cells in culture where the amount of material is not limiting. Alternatively, investigators can efficiently dissect cancer cells from a study set of cases to assess the frequency of particular molecular profiles across large control and analysis groups. One can also envision xMD being employed as a component of current commercially available laser dissection instruments, combining rapid and precise dissection of xMD with the useful features (image archiving, phenotype-based dissection) of these systems.

ACKNOWLEDGMENTS

Expression microdissection was initially described in NIH employee invention report E-100-2001/0 (January, 2001; Emmert-Buck, MR) and is the subject of two United States and international patent applications. The authors thank Dr. Mark Raffeld and Dr. Elizabeth Woodhouse for their technical assistance on the project. The present manuscript is dedicated to the memory of Dr. Benedicto Chuaqui, Full Professor, Department of Pathology, Catholic University, Santiago, Chile; Member, Chilean Academy of Medicine; and Member, Academy of Science, Heidelberg, Germany. We trust that the study is in keeping with Benedicto Chuaqui's constant pursuit of truth through knowledge.

REFERENCES

1. Fearon ER, Hamilton SR, Vogelstein B. Clonal analysis of human colorectal tumors. *Science*. 1987;238:193–197.
2. Shibata D, Hawes D, Li ZH, et al. Specific genetic analysis of microscopic tissue after selective ultraviolet radiation fractionation and the polymerase chain reaction. *Am J Pathol.* 1992;141:539–543.
3. Radford D, Fair K, Thompson AM, et al. Allelic loss on a chromosome 17 in ductal carcinoma in situ of the breast. *Cancer Res*. 1993;53:2947–2949.
4. Emmert-Buck MR, Roth MJ, Zhuang Z, et al. Increased gelatinase A (MMP-2) and cathepsin B activity in invasive tumor regions of human colon cancer samples. *Am J Pathol.* 1994;145:1285–1290.
5. Zhuang Z, Bertheau P, Emmert-Buck MR, et al. A microdissection technique for archival DNA analysis of specific cell populations in lesions < 1 mm in size. *Am J Pathol*. 1995;146:620–625.
6. Going J, Lamb RF. Practical histological microdissection for PCR analysis. *Am J Pathol*. 1996;179:121–124.
7. Moskaluk CA, Kern SE. Microdissection and polymerase chain reaction amplification of genomic DNA from histological tissue sections. *Am J Pathol.* 1997;150:1547–1552.
8. Becker I, Becker K, Rohrl MH, et al. Laser-Assisted Preparation of Single Cells from Stained Histological Slides for Gene Analysis. *Histochem Cell Biol*. 1997;108:447–451.
9. Bohm M, Wieland I, Schutze K, et al. Non-contact laser microdissection of membrane-mounted native tissue. *Am J Pathol*. 1997;151:63–67.
10. Schutze K, Lahr G. Identification of expressed genes by laser-mediated manipulation of single cells. *Nat Biotechnol.* 1998;16:737–740.
11. Luo L, Salunga RC, Guo H, et al. Gene expression profiles of laser-captured adjacent neuronal subtypes. *Nat Med*. 1999;5:117–122.
12. Emmert-Buck MR, Bonner RF, Smith PD, et al. Laser capture microdissection. *Science*. 1996;274:998–1001.
13. Bonner RF, Emmert-Buck MR, Cole KA, et al. Laser capture microdissection: Molecular analysis of tissue. *Science*. 1997;278:1481–1483.
14. Rubin M. Understanding disease cell by cell. *Science*. 2002;296:1329–1330.
15. Murakami H, Liotta L, Star RA. IF-LCM: Laser capture microdissection of immunofluorescently defined cells for mRNA analysis rapid communication. *Kidney Int*. 2000;58:1346–1353.
16. Chuaqui RF, Englert CR, Strup SE, et al. Identification of a novel transcript up-regulated in a clinically aggressive prostate carcinoma. *Urology*. 1997;50:302–307.
17. Ornstein DK, Gillespie JW, Paweletz CP, et al. Proteomic analysis of laser capture microdissected human prostate cancer and in vitro prostate cell lines. *Electrophoresis*. 2000;21:2235–2242.
18. Zhou M, Shah R, Shen R, et al. Basal cell cocktail (34betaE12 + p63) improves the detection of prostate basal cells. *Am J Surg Pathol*. 2003;3:365–371.
19. Ahram M, Flaig MJ, Gillespie JW, et al. Evaluation of ethanol-fixed, paraffin-embedded tissues for proteomic applications. *Proteomics*. 2003;3:413–421.
20. Leiva IM, Emmert-Buck MR, Gillespie JW. Handling of clinical tissue specimens for molecular profiling. *Curr Issues Mol Biol*. 2003;5:27–35.

